Image registration and mutual thresholding enable low interimage variability across dynamic MRI measurements of supraclavicular brown adipose tissue during mild cold exposure

Mishre, A.S.D.S.; Martinez-Tellez, B.; Straat, M.E.; Boon, M.R.; Dzyubachyk, O.; Webb, A.G.; ... ; Kan, H.E.

Received: 6 December 2022 | Revised: 26 April 2023 | Accepted: 27 April 2023 | Published on: 15 May 2023

DOI: 10.1002/mrm.29707

RESEARCH ARTICLE

Magnetic Resonance in Medicine

Image registration and mutual thresholding enable low interimage variability across dynamic MRI measurements of supraclavicular brown adipose tissue during mild cold exposure

Aashley S. D. Sardjoe Mishre[1,2,3] | **Borja Martinez-Tellez**[1,2] | **Maaike E. Straat**[1,2] | **Mariëtte R. Boon**[1,2] | **Oleh Dzyubachyk**[4,5] | **Andrew G. Webb**[3] | **Patrick C. N. Rensen**[1,2] | **Hermien E. Kan**[3]

[1]Department of Medicine, Division of Endocrinology, Leiden University Medical Center, Leiden, the Netherlands

[2]Einthoven Laboratory for Experimental Vascular Medicine, Leiden University Medical Center, Leiden, the Netherlands

[3]Department of Radiology, C.J. Gorter MRI Center, Leiden University Medical Center, Leiden, the Netherlands

[4]Department of Radiology, Division of Image Processing, Leiden University Medical Center, Leiden, the Netherlands

[5]Department of Cell and Chemical Biology, Electron Microscopy Section, Leiden University Medical Center, Leiden, the Netherlands

Correspondence
Hermien E. Kan, Department of Radiology, C.J. Gorter MRI Center, Leiden University Medical Center, Leiden, the Netherlands.
Email: h.e.kan@lumc.nl

Funding information
Netherlands Cardiovascular Research Initiative, Grant/Award Number: CVON2017; NWO, Grant/Award Number: 09150161910073

Purpose: Activated brown adipose tissue (BAT) enhances lipid catabolism and improves cardiometabolic health. Quantitative MRI of the fat fraction (FF) of supraclavicular BAT (scBAT) is a promising noninvasive measure to assess BAT activity but suffers from high scan variability. We aimed to test the effects of coregistration and mutual thresholding on the scan variability in a fast (1 min) time-resolution MRI protocol for assessing scBAT FF changes during cold exposure.

Methods: Ten volunteers (age 24.8 ± 3.0 years; body mass index 21.2 ± 2.1 kg/m^2) were scanned during thermoneutrality (32°C; 10 min) and mild cold exposure (18°C; 60 min) using a 12-point gradient-echo sequence (70 consecutive scans with breath-holds, 1.03 min per dynamic). Dynamics were coregistered to the first thermoneutral scan, which enabled drawing of single regions of interest in the scBAT depot. Voxel-wise FF changes were calculated at each time point and averaged across regions of interest. We applied mutual FF thresholding, in which voxels were included if their FF was greater than 30% FF in the reference scan and the registered dynamic. The efficacy of the coregistration was determined by using a moving average and comparing the mean squared error of residuals between registered and nonregistered data. Registered scBAT ΔFF was compared with single-scan thresholding using the moving average method.

Results: Registered scBAT ΔFF had lower mean square error values than nonregistered data (0.07 ± 0.05% vs. 0.16 ± 0.14%; $p < 0.05$), and mutual thresholding reduced the scBAT ΔFF variability by 30%.

Conclusion: We demonstrate that coregistration and mutual thresholding improve stability of the data 2-fold, enabling assessment of small changes in FF following cold exposure.

KEYWORDS
brown adipose tissue, cold exposure, fat fraction, magnetic resonance imaging

1 | INTRODUCTION

Brown adipose tissue (BAT) is a thermogenic tissue that metabolizes fatty acids and glucose into heat. The most potent activator of BAT is cold exposure, upon which norepinephrine is released by sympathetic nerve endings in BAT. Norepinephrine binds to β-adrenergic receptors on the brown adipocytes and activates a thermogenic program, including intracellular lipolysis and short circuiting of the electron transport chain by the uncoupling protein 1.[1] Intracellular lipid stores are subsequently replenished by extracting lipids and glucose from the blood.[2] Because BAT is involved in lipid and glucose metabolism, many studies have addressed its protective role against obesity and cardiometabolic diseases.[3–6] This tissue is known to be activated not just by cold exposure,[7] but also by drugs like the β2-adrenergic receptor agonist salbutamol.[8]

BAT activity during such challenges is usually indirectly assessed by quantifying the glucose uptake of the radioactively labeled glucose analogue [^{18}F]fluorodeoxyglucose, using PET/CT.[9] However, [^{18}F]fluorodeoxyglucose PET-CT depends on ionizing radiation, which increases the participation burden and hampers longitudinal studies. In addition, this modality visualizes the glucose uptake, while BAT predominantly metabolizes lipids rather than glucose.[10] Most importantly, glucose uptake by BAT is reduced in individuals who are insulin resistant, such as in obesity and type 2 diabetes; therefore, the technique is much less reliable in these patients.[10]

MRI is a noninvasive and safe method for estimating supraclavicular BAT (scBAT) activity during cold exposure using chemical shift–based water-fat separation sequences, such as the Dixon technique, for quantitative fat fraction (FF) mapping.[11] In previous studies, cold-induced supraclavicular FF changes between −0.4 and −3.5% have been reported.[11,12] Most of these studies have either used pre-cooling and post-cooling assessments of scBAT FF[12] or have been performed without the use of image registration[13,14] or breath-holds.[15–17] Because scBAT is located in the supraclavicular area, rendering measurements prone to movement artifacts, dynamic scans may yield more reliable scBAT ΔFF measurements, as pre-cooling and post-cooling assessments do not capture the variability in between time points. In addition, most studies acquired images at a relatively coarse temporal resolution of 2.5–5 min.[13,17,18] It has been shown, however, that BAT activation occurs within 10 min after applying a cold stimulus.[13,19] For instance, Reber et al. showed an increase in oxygen-saturated hemoglobin levels that was detected in the supraclavicular region within 10 min after activation.[19] In addition, Oreskovich et al. showed that scBAT FF decreased significantly after only 10 min of cooling.[13] Hence, a coarse time resolution of 5 min may not be sufficient to study the short-time dynamics of BAT in detail.

Here, we aimed to minimize interscan variability by applying breath-holds and nonrigid image registration in a MRI protocol with a high temporal resolution for assessing FF dynamics in scBAT during cold exposure.

2 | METHODS

2.1 | Subjects

Ten healthy volunteers with an age between 18 and 25 years and a body mass index (BMI) between 18 and 25 kg/m^2 were recruited from our local healthy volunteer database and by using flyers. Exclusion criteria were the use of any medication known to affect lipid and/or glucose metabolism, recent excessive weight change, smoking, and contra-indications for MRI. The study was performed in accordance with the Declaration of Helsinki and was approved by the local medical ethics committee. Written consent was obtained from all participants before participation.

2.2 | Study design and cooling protocol

Participants were instructed to fast overnight for 12 h and to withhold from alcohol and caffeine consumption for 24 h before the experiment. On the day of the experiment, participants were asked to wear a t-shirt, shorts, and slippers. Body weight and height were measured, and BMI was calculated by dividing the body weight by height squared (kg/m^2). Participants then entered the MRI suite and were positioned on the MR table. A water circulating blanket (Blanketrol III hyper-hypothermia system; Cincinnati Sub-Zero, Cincinnati, OH, USA) was placed on top of the participant, and the temperature was initially set to 32°C. After 10 min at thermoneutrality, data were acquired for 10.5 min before the temperature was lowered to 18°C to initiate the standardized cooling protocol for BAT activation (Figure 1). Every 10–15 min, participants were asked to score their cold perception using a numeric rating scale (NRS; 1 = comfortable and 10 = extremely cold). The total cooling duration was 63 min. The experiment was stopped in case of self-reported shivering. Scans were conducted at the same time of day in all participants (10:30 a.m.–12.00 p.m.) between April 16 and July 23, 2021.

2.3 | Image acquisition

Data were acquired on a 3T MRI scanner (Philips Ingenia Elition X; Philips Healthcare, Best, the Netherlands)

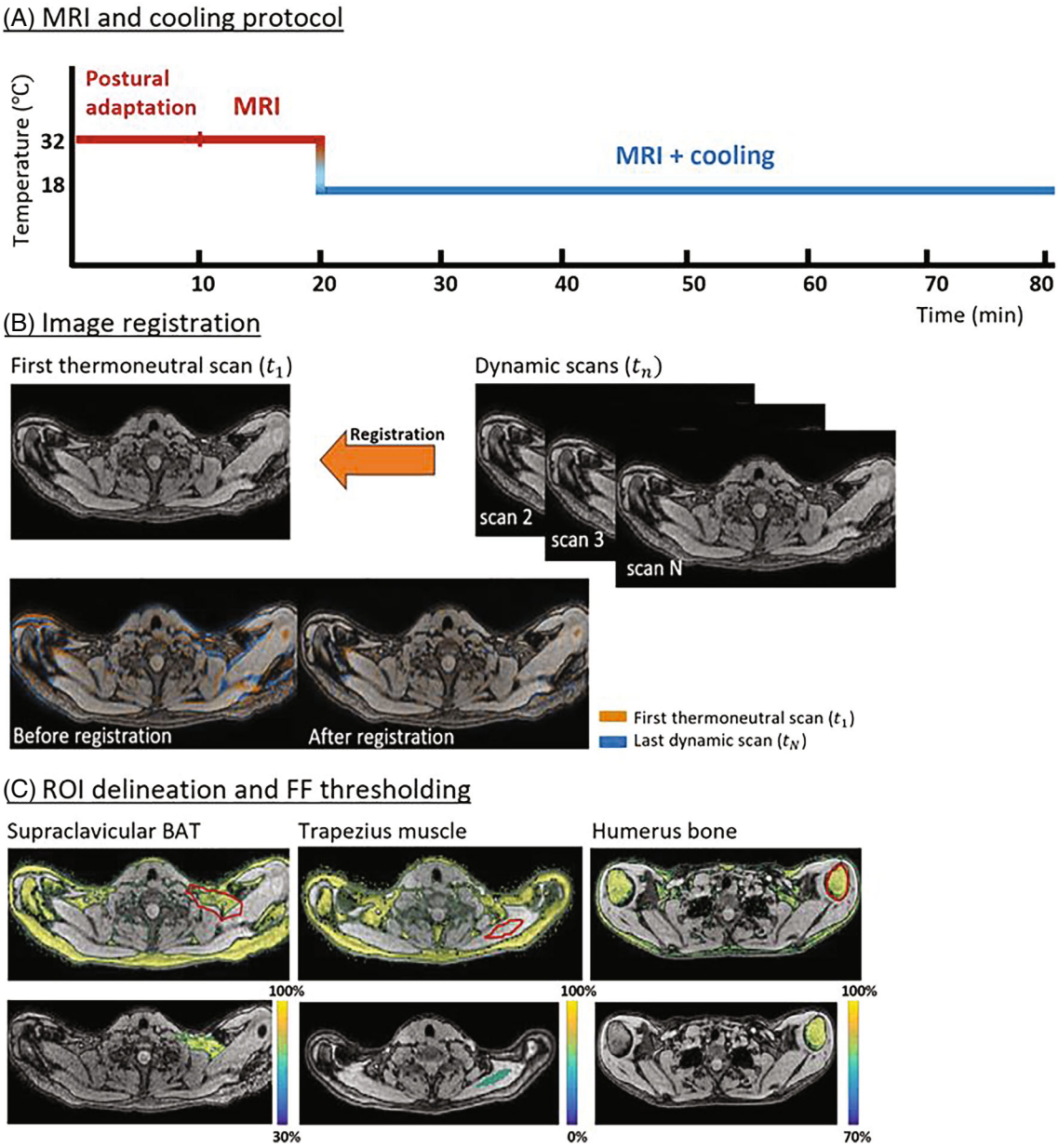

FIGURE 1 (A) Participants underwent a standardized cooling protocol to activate brown adipose tissue (BAT). After 20.5 min at thermoneutrality (32°C), the temperature was set to 18°C for 63 min. Images were acquired during the last 10.5 min at thermoneutrality and during cooling. (B) The first thermoneutral scan was used as a reference image, and all subsequent dynamic scans were coregistered to the first scan. First-echo magnitude images were used for coregistration, and the resulting transformation was used to deform the fat fraction (FF) map of each dynamic to match the image coordinates of the first thermoneutral scan. (C) Regions of interest (ROIs) were only drawn on the first thermoneutral scan, and voxels below 30% FF were mutually excluded in both fixed and dynamic scans to avoid inclusion of nonfatty tissue for supraclavicular BAT (scBAT). No FF thresholds were used for muscle, and a 70%–100% mutual FF threshold range was used for the humerus bone.

using a 16-channel head-and-neck coil, a 12-channel phased array placed on top of the subject, and an in-table 16-channel array for signal reception. A 3D multi-gradient-echo sequence with 12 echoes (mDIXON Quant) was used with the following parameters: TR = 12 ms, first TE = 1.12 ms, echo time separation ΔTE = 0.87 ms, flip angle = 3°, FOV = 400 × 229 × 134 mm^3 (right–left, feet–head, anterior–posterior), 2.1-mm isotropic resolution, and breath-hold time of 16 s. We used 12 echoes to support a reliable T_2^* decay estimation.[20] The acquisition time per scan was 1.05 min, which yielded a total of 70 scans: 10 scans at thermoneutrality and 60 scans during cooling.

To evaluate the stability of the sequence over time, a commercial phantom that consisted of 12 water-fat emulsion tubes (Calimetrix[21]) with low FFs (0%, 2.7%, 5.3%,

and 7.8%), intermediate FFs (10.1%, 15.5%, 20.4%, and 23.6%), and high FFs (30.2%, 39.9%, 50.1%, and 100%) was scanned for 1 h at room temperature using a 16-channel head-and-neck coil with the previously described parameter settings.

2.4 | Water-fat data reconstruction

An in-house-developed complex-based fitting algorithm was used to estimate voxel-based water and fat signals based on the known frequencies and amplitudes of the multipeak lipid spectrum and accounting for the mono-exponential decay (T_2^*) of both water and fat components.[22] The field inhomogeneity map obtained from the mDIXON Quant sequence was used as an initial estimate in the water-fat separation model. FF maps were subsequently calculated by dividing the fat signal by the sum of the water and fat signals in each voxel across the 3D image.

2.5 | Phantom data analysis

For analysis of the phantom data, a region of interest (ROI) was manually delineated for each phantom tube on the first scan. A single rectangular ROI was placed in the middle of each tube, and ROIs were transferred directly to all subsequent dynamic scans. For each tube, voxel-wise FF differences between the first scan and each dynamic scan i, $\Delta FF_i(x, y, z) = FF_i(x, y, z) - FF_1(x, y, z)$, were computed and averaged across the ROI.

2.6 | In vivo image registration and ROI segmentation

For analysis of the in vivo data, first-echo magnitude images of each dynamic were coregistered to the first thermoneutral scan (reference scan) using the open-access registration toolbox Elastix[23] (Figure 1B). Dynamic images were iteratively deformed using a 3D B-spline on a $10 \times 10 \times 10\,mm^3$ grid, adaptive stochastic gradient descent with two resolutions, 4000 iterations, and the Mattes mutual information as the similarity metric.[24] As a result, ROIs only needed to be delineated on the first thermoneutral scan. ROIs were coarsely delineated in the scBAT depot, and we applied a mutual FF thresholding approach, in which voxels were only included in the analysis if their FF was above 30% in both the reference scan and the registered dynamic. As a control, ROIs were also drawn in the trapezius muscle and the humeral bone using 0%–100% and 70%–100% mutual FF threshold levels, respectively. Voxel-wise FF differences between the reference scan and each dynamic scan i, $\Delta FF_i(x, y, z) = FF_i(x, y, z) - FF_{TN1}(x, y, z)$, were calculated and averaged across the ROI.

2.7 | Data analysis and statistics

The following analyses were performed to (i) determine the stability of the high-temporal-resolution MRI protocol, (ii) evaluate the validity and added value of image registration, (iii) evaluate the added value of mutual FF thresholding, and (iv) compare cold-induced scBAT FF changes with control tissues.

2.7.1 | Stability of the high-temporal-resolution MRI protocol in the phantom

The effect of RF heating and gradient-induced heating[25–27] on the temporal stability of the MRI protocol was evaluated by assessing temporal FF changes in each phantom tube. Temporal FF changes were fitted by a linear equation. To quantify any decreasing or increasing trends, the vertical distance between the last and the first point along the fitted trend line was determined.

Next, a moving average was computed along the FF changes of each phantom tube using a [−3,3] time window. As a measure of the variability, the mean squared error (MSE) of residuals between the moving average and the measured FF data was calculated. This method will be further referred to as the "moving average method."

2.7.2 | Evaluating the validity and added value of coregistration of in vivo data

For each subject, we first estimated the X, Y, and Z displacement of each dynamic with respect to the reference scan (Figure S1) to assess slight differences in positioning. We then translated and registered the first thermoneutral (reference) scan to the dynamics to mimic the same extent of motion in the reference scan. This yielded a forward transformation (reference➔dynamic) for each dynamic. To study the influence of small positional changes due to motion on scBAT FF changes, FF differences were calculated for each time point between the original reference scan's FF values and the deformed reference scan's FF values and averaged across the scBAT ROI. Each dynamic scan was subsequently registered to the reference scan to obtain the backward transformation matrix (dynamic➔reference). For each dynamic, the forward and

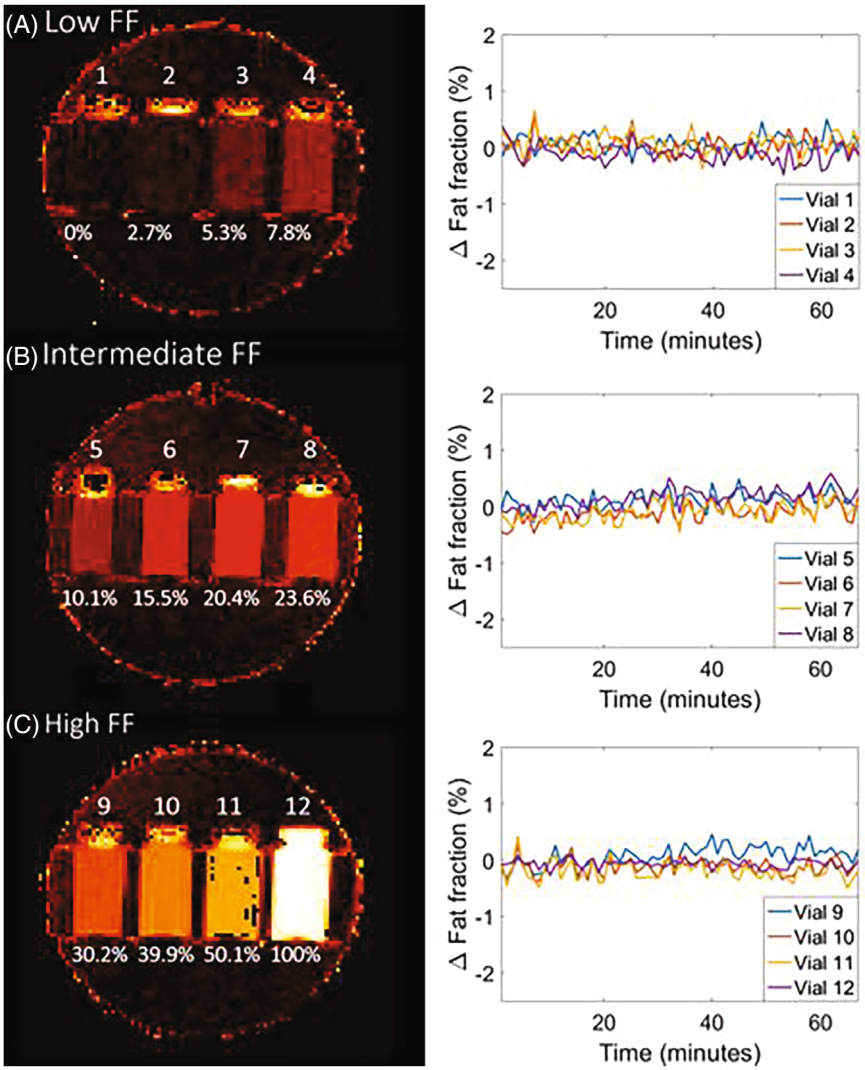

FIGURE 2 Fat fraction (FF) changes are plotted as a function of time for water-fat emulsion tubes in the low FF range (0%, 2.7%, 5.3%, 7.8%) (A), intermediate FF range (10.1%, 15.5%, 20.4%, 23.6%) (B), and high FF range (30.2%, 39.9%, 50.1%, 100%) (C).

the backward transformations were composed and applied to the reference scan to correct for the motion-induced variability. FF difference maps were generated between the resulting deformed reference scan and the original one. For each time point, voxel-wise FF differences between the original reference scan and the deformed one were computed, $\Delta FF_{error}(x, y, z) = FF_{def}(x, y, z) - FF_{TN1}(x, y, z)$, and averaged across the ROI in the scBAT area. To quantify any decreasing or increasing trends of the registration error, a trendline was fitted along the ΔFF_{error} time series for each participant. As a measure of the variability along the ΔFF_{error} time series, MSE values were computed for each participant using the moving average method. The influence of small positional changes due to motion on FF changes, as well as motion-corrected FF changes, are visualized in Figure S2 for supraclavicular BAT, the trapezius muscle, and the humerus bone.

The added value of the coregistration method was determined by comparing scBAT FF changes during cold exposure between registered and nonregistered data. The moving average method was used to determine the variability of scBAT ΔFF obtained from registered and nonregistered data for each participant separately, as a measure for the intrasubject variability. Paired t-tests were performed to compare the intrasubject variability between registered and nonregistered data.

2.7.3 | Evaluating the added value of mutual FF thresholding of in vivo data

The added value of mutual FF thresholding was assessed by comparing scBAT FF changes obtained from mutual and single FF thresholding using the moving average method. Single FF thresholding was performed by applying a 30%–100% FF threshold to each individual dynamic. Data were analyzed separately for registered and nonregistered scBAT FF changes, and paired t-tests were performed to compare the intrasubject variability between mutual and single FF thresholded data.

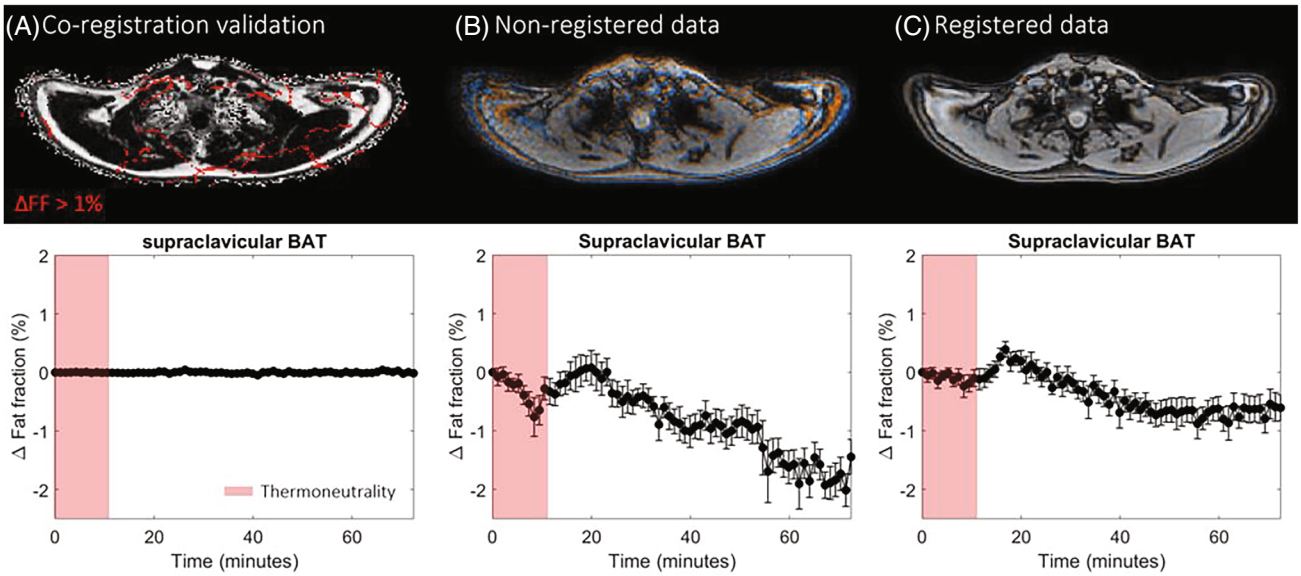

FIGURE 3 Fat fraction changes for the coregistration validation analysis (A), nonregistered data (B), and registered data (C). Supraclavicular brown adipose tissue (BAT) fat fraction changes above 1% are shown in red in (A). Image overlap between the first thermoneutral (reference) scan and the last dynamic are shown for (B) and (C), where the reference scan and the last dynamic are shown in orange and blue, respectively. Red denotes thermoneutrality. Data are presented as mean ± SEM for all 10 subjects.

2.7.4 | Comparing the scBAT FF response to control tissues (skeletal muscle and humerus bone)

Next, it was determined whether the scBAT FF changes over time differed from those estimated in control tissues: the trapezius muscle and the humerus bone. The moving average method was used to determine the variability of FF for both control tissues. Afterward, the ΔFF time series of each control tissues were subtracted from the scBAT ΔFF time series, which yielded two difference curves: ΔFF_{scBAT}-$\Delta FF_{trapezius}$ and ΔFF_{scBAT}-$\Delta FF_{humerus}$. To prevent overestimation of the statistical power, FF differences were averaged across every 10 scans along the measurement interval, resulting in seven temporal measurements. For each control tissue, it was determined whether the difference curve deviated from zero using a mixed model analysis. Thermal perception scores were compared between thermoneutrality and each cooling period using the Wilcoxon signed-rank test. Data analysis was performed using *MATLAB* (version R2021a) and *SPSS*. Results were considered significant at $p < 0.05$.

3 | RESULTS

Ten young and lean subjects (age = 24.8 ± 3.0 years and BMI = 21.2 ± 2.1 kg/m^2) participated. Nine participants were female, and 1 participant was male. All participants completed the protocol. Participants reported significantly higher cold perceptions compared with thermoneutrality (NRS = 1.5 ± 0.7) after 16.25 min of cooling (NRS = 3.7 ± 1.0; $p = 0.004$), 32 min of cooling (NRS = 3.6 ± 0.9; $p = 0.005$), 47.75 min of cooling (NRS = 3.6 ± 1.1; $p = 0.007$), and after 63 min of cooling (NRS = 4.1 ± 1.3; $p = 0.005$).

Phantom tubes with low, intermediate, and high FFs showed stable ΔFF measurements over time (Figure 2A–C). The vertical distance along the fitted trendlines was −0.05 ± 0.08% for the low FF tubes, 0.27 ± 0.10% for the intermediate FF tubes, and 0.05 ± 0.20% for the high FF tubes. The MSE values were 0.02 ± 0.005% for the low FF tubes, 0.02 ± 0.005% for the intermediate FF tubes, and 0.02 ± 0.01% for the high FF tubes.

The coregistration error caused substantially small FF changes over time (MSE: 0.001 ± 0.002%; Figure 3A) and resulted in a vertical distance of 0.003 ± 0.001% along the fitted trendlines. The intrasubject MSE values of registered scBAT ΔFF were lower compared with those for nonregistered data (MSE: 0.07 ± 0.05% vs. MSE: 0.16 ± 0.14%, respectively; $p = 0.01$; Figure 3B,C) and resulted in an increase in the ΔFF response over time by a factor of two.

For nonregistered data, mutual FF thresholding on average increased the MSE values compared with single FF thresholding (0.16 ± 0.14% vs. 0.13 ± 0.13%; $p = 0.01$; Figure 4A). For registered data, mutual FF thresholding on average reduced the MSE values compared with single FF thresholding; however, this was not significant (MSE: 0.07 ± 0.05% vs. MSE: 0.10 ± 0.10%; $p = 0.1$; Figure 4B). The results of the coregistration experiment are presented in

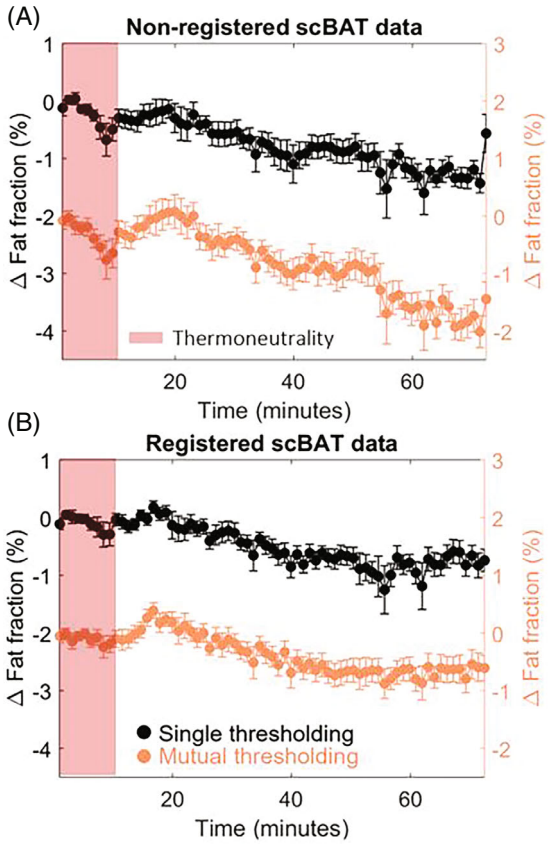

FIGURE 4 Fat fraction (FF) changes are shown for nonregistered data (A) and registered data (B) after applying a 30%–100% single FF threshold (black) and mutual FF threshold (orange). Red denotes thermoneutrality. Data are presented as mean ± SEM for all 10 subjects. scBAT, supraclavicular brown adipose tissue.

Figure 5 for all participants, and results obtained from the nonregistered data are presented for all individuals in Figure S3.

As expected, FF changes in the trapezius muscle and the humerus bone revealed no specific FF patterns during cooling with small changes over time (skeletal muscle MSE: 0.05 ± 0.05% and humerus bone MSE: 0.11 ± 0.06%; Figure 6A,B). ΔFF in scBAT was significantly reduced by −0.68 ± 0.76%, −0.80 ± 0.88%, and − 0.66 ± 0.81% compared with ΔFF in the trapezius muscle at time intervals 5 (43–53 min), 6 (54–63 min), and 7 (64–73 min), respectively. Compared with the humerus bone, scBAT ΔFF was significantly reduced by −0.39 ± 0.61% and −0.43 ± 0.46% at time intervals 5 and 6 (Figure 6C).

4 | DISCUSSION

In this work, we developed a 1-min time-resolution protocol for the assessment of scBAT FF changes using breath-holds and coregistration to minimize motion-induced variation. Our MRI protocol showed a high stability of FF in the phantom, and coregistration and mutual FF thresholding of in vivo data improved stability of scBAT FF changes compared with nonregistered data. On average, cold exposure first increased scBAT FF, followed by a gradual decrease, compared with control tissues. This trend was observed in four out of 10 participants.

Our MRI protocol resulted in a low variability of less than 0.1% FF in all phantom tubes over the entire scan duration of 70 min. No FF trend of 0.5% or higher occurred in any of the phantom tubes. In previous work, similar results were found regarding the repeatability of FF measurements in the Calimetrix phantom,[21] in which a FF difference of 0.8% or lower between measurements that were performed on three different occasions was shown. Our data additionally show that the stability across FF measurements is maintained while acquiring images consecutively for 63 min using a 1-min temporal resolution. As such, influences from the scanner's hardware, such as B_0 drift, appear to have a minimal effect on the temporal stability of the FF measurements.

The coregistration method achieved a high registration accuracy on the in vivo data, indicated by the absence of any temporal pattern of the registration error and small FF changes over time. The data, in which motion was mimicked, had an MSE value of 0.15 ± 0.11% and a vertical distance of 0.50 ± 1.41% (Figure S2A) in the scBAT area, whereas the variability was substantially reduced after correcting for motion (MSE: 0.001 ± 0.002% and vertical distance = 0.003 ± 0.001%; Figure 3A and Figure S2D). Similar results were found for the trapezius muscle and humerus bone (Figure S2). Due to the location of BAT in the supraclavicular area, the measurements are especially prone to movement artifacts. Indeed, our data show that coregistration reduces the intrasubject variability 2-fold compared with nonregistered data while using mutual FF thresholding. This translated, on average, to double the scBAT FF reduction during cooling for nonregistered data compared with registered data.

For nonregistered data, mutual FF thresholding increased the intrasubject variability by 23% compared with single FF thresholding. This increase is the result of large spatial mismatches between the reference scan and nonregistered dynamics, which reduces the number of colocated voxels with a FF above 30% in both the reference scan and dynamic, thereby confirming the presence of motion across the dynamics. For registered data, mutual FF thresholding reduced the intrasubject variability by 30% compared with single-FF-thresholded data. Because the spatial mismatches between the reference scan and registered dynamics are mostly resolved, the mutual thresholding approach only accounts for small spatial

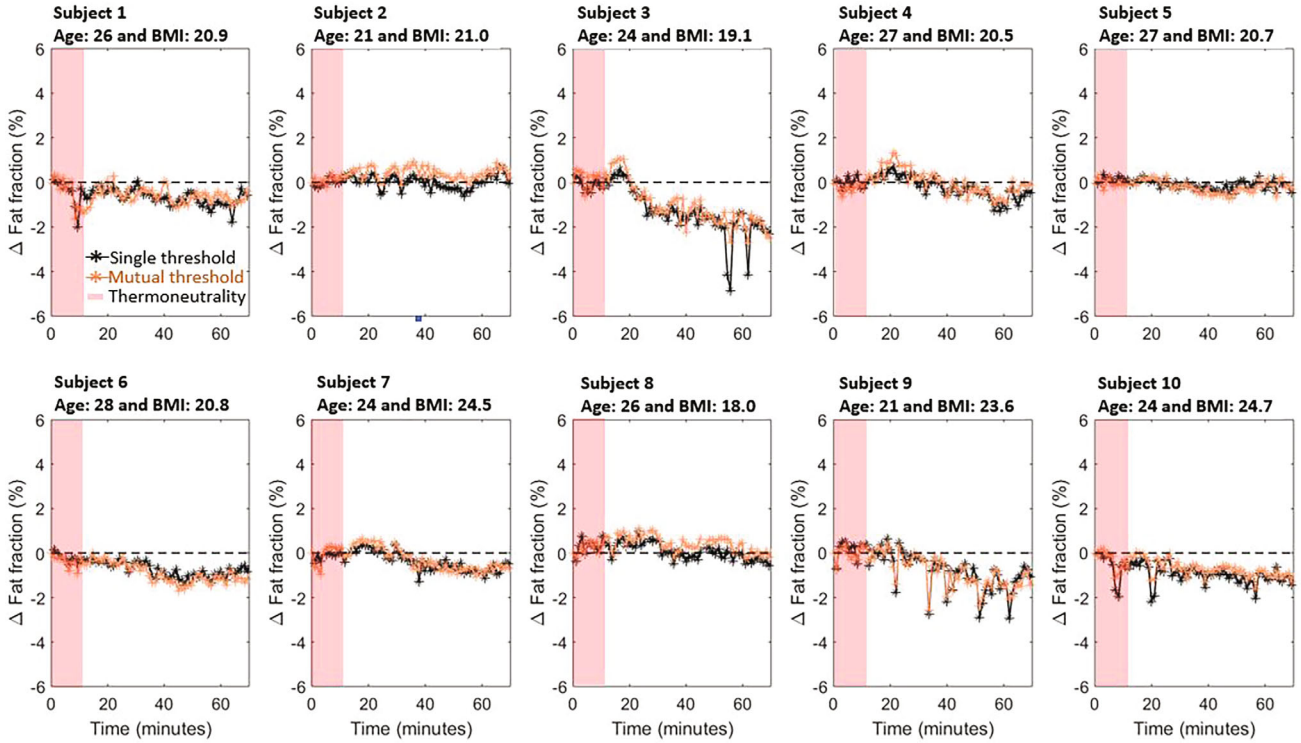

FIGURE 5 Fat fraction (FF) changes are shown for registered data after applying a 30%–100% single FF threshold (black) and mutual FF threshold (orange). Red boxes denote the thermoneutral period. Data are shown for all participants, including their age (years) and body mass index (BMI) (kg/m^2).

mismatches between scans that are still present after the registration, such as partial volume effects.

The added value of the coregistration is less pronounced when comparing registered and nonregistered data obtained with single FF thresholding, in which the intrasubject variability was reduced by 23%. Nevertheless, by combining image registration and mutual FF thresholding, the intrasubject variability of scBAT ΔFF (MSE: $0.07 \pm 0.05\%$) was further reduced by almost 2-fold compared with nonregistered data obtained with single FF thresholding (MSE: $0.13 \pm 0.13\%$) and mutual FF thresholding (MSE: $0.16 \pm 0.14\%$). Our results, therefore, highlight the importance of using both methods for these kinds of tissue types that are prone to motion artifacts.

Compared with the studies in which scans were obtained during cooling, our scBAT FF changes are generally smaller (−1.94%,[16] −2.9%,[18] −3.0%,[13,14] −3.5%,[24] and −4.7%[15]). This could be due to several reasons, including the lack of breath-holds and/or coregistration or differences in previous study protocols. As a result, the reported scBAT FF changes may have been overestimated as a result of motion. Several studies did use coregistration in their analysis[15–17]; however, images were acquired during free breathing. Because the registration error increases with the amount of image deformation,[28] it cannot be excluded that this may have influenced the outcomes. A previous study by Stahl et al. used both image registration and breath-holds in their protocol[18]; however, images were acquired using a 2-echo Dixon protocol. It has been shown that a 2-echo sequence overestimates the FF below 60% and underestimates the FF above 60% compared with a 6-echo protocol,[29] which is the result of field inhomogeneities that are not corrected, therefore producing misleading scBAT ΔFF outcomes.

Moreover, differences in the applied cooling procedures (e.g., cooling garments, duration, intensity, medium) (i.e., water or air) or strategy (i.e., personalized or standardized) may also have contributed to the inconsistency in FF outcomes in the literature. Although participants reported an increased cold perception during cooling, a larger ΔFF scBAT response may have occurred in previous studies,[14,15,24] as participants were exposed to lower temperatures compared with our standardized mild-cooling protocol (18°C). Because no thermal perception scores were reported in these previous studies, this hypothesis should be further tested by comparing thermal perception measurements and scBAT ΔFF outcomes across different cooling procedures.

Overall, scBAT FF changes were found to be significantly reduced with respect to the control tissues during the last 30 min of cooling. This gradual decrease in scBAT FF is most likely attributed to the lipolysis within the

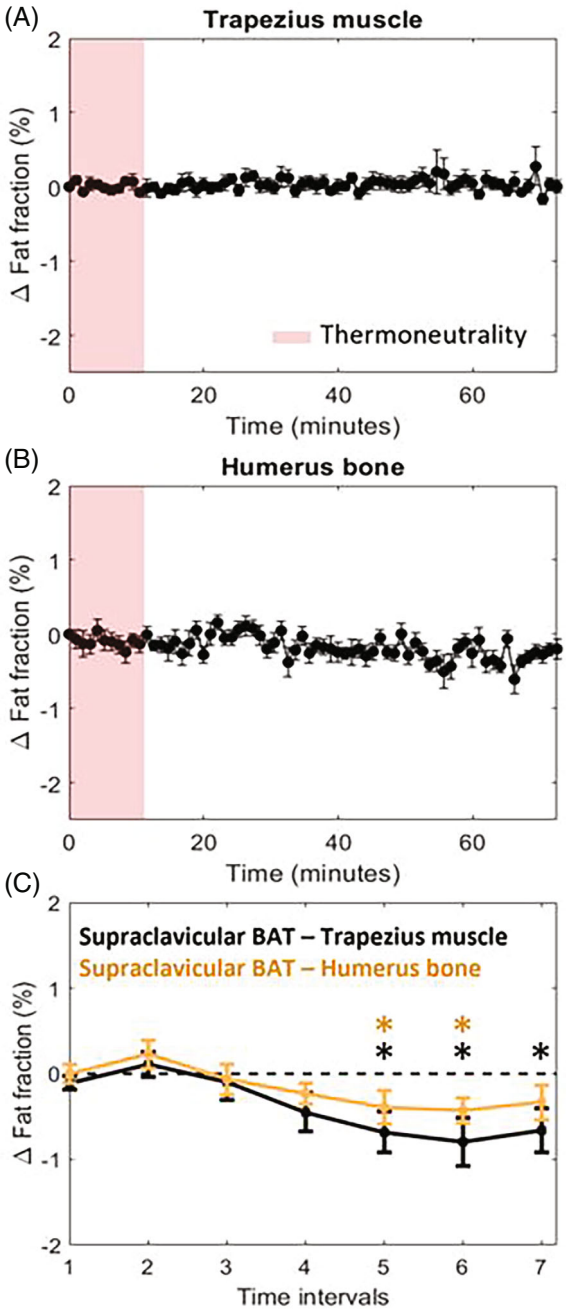

FIGURE 6 (A,B) Fat fraction (FF) changes for the trapezius muscle and humerus bone. (C) FF difference curves between supraclavicular brown adipose tissue (BAT), the trapezius muscle (black), and the humerus bone (orange). The FF difference curves are averaged across every 10 scans along the measurement, which yielded seven temporal intervals. Data are presented as mean ± SEM for all 10 subjects. *$p < 0.05$.

scBAT depot. While an increase in perfusion could produce a change in image intensity, leading to an apparent reduction in scBAT FF, this seems unlikely for several reasons. First, Blondin et al. showed that BAT perfusion determined by ^{11}C-acetate PET-CT was unaltered after 3 h of cold exposure in healthy adults, and that intracellular triglycerides were the primary fuel for BAT thermogenesis.[1] Second, Coolbaugh et al. reported a mean FF decrease of 14% in voxels with a FF in the 90%–100% decade after 1 h of personalized cold exposure.[15] The authors argued that, if half of the water signal came from blood at thermoneutrality (e.g., assuming a blood volume fraction of 2.5% at baseline), then the blood volume fraction would have increased by 16.5% to explain this reduction of 14%, which is very unlikely. In addition, Lundstrom et al. showed that the reduction in scBAT FF determined by MRI persisted after the cooling was removed, which argues against perfusion being a dominant factor because it would then be expected that the perfusion would decrease.[16] Finally, the gradual FF increase (+0.4% FF) at the onset of cooling is not in line with a major role of perfusion, as increased perfusion would be accompanied by an apparent immediate decrease in scBAT FF due to the increased volume fraction of water.

To the best of our knowledge, the small increase in FF after cooling we observed has not been reported before but could be due to lipid uptake in scBAT from the blood before lipolysis. This would be in line with recent data from Straat et al., who showed that plasma triglyceride levels transiently decreased in response to cold exposure.[30] We postulate that soon after the initiation of cold exposure, BAT rapidly increases the uptake op triglyceride-derived fatty acids, resulting in the observed initial scBAT FF increase. Then, after 8 min, the lypolysis of intracellular lipids possibly exceeds the uptake of fatty acids, leading to an overall decrease in scBAT FF. Future research could, therefore, combine these measures with repeated blood sampling to experimentally address this hypothesis. In line with previous reports,[15,24] we showed that the scBAT FF response is very heterogenous (Figure S4), in which scBAT FF increased in lipid-poor regions and decreased in lipid-rich regions after cooling. This potentially varying net flux of lipids due to lipolysis and lipid uptake may therefore explain the relatively small net effect and could partly explain the variability of scBAT FF across measurements.

This study has several limitations. We referred to supraclavicular fat fraction as scBAT FF, yet it should be noted that the supraclavicular depot is a mixture of both BAT and white adipose tissue, and because of the relatively low image resolution, classical BAT cannot be differentiated from white adipose tissue. In addition, scBAT FF changes may have been influenced by the lack of specificity to identify BAT within the supraclavicular depot due to the limited resolution of MRI and partial volume effects. In our protocol, 140 breath-holds of 16 s were required from the subject, which would constitute a high burden when applied in patients. Because our data showed an interimage variability (MSE) of less than 0.1% in scBAT, this may allow the use of lower temporal resolutions at

intervals for which scBAT FF changes are stable (e.g., thermoneutrality or prolonged cooling[13]). Another limitation is that the study population only included young and healthy adults and one male; therefore, our results cannot be extrapolated to a more general population. Moreover, the absolute change in FF is relatively small; thus, further research is required to determine whether this small change can be used to detect differences between groups of individuals and patients with varying amounts of active BAT. Ideally, our measurements should have been performed with a "negative control" experiment: an additional session without cooling using the same experimental conditions. Future research is needed to further assess the physiological mechanisms that may drive scBAT FF changes by comparing these changes to control measurements and other techniques, such as plasma lipid measurements.

5 | CONCLUSION

Coregistration and mutual thresholding improve stability of the data 2-fold, enabling assessment of small changes in FF following cold exposure. These motion-correcting techniques are therefore highly recommended to improve the stability of scBAT ΔFF measurements.

ACKNOWLEDGMENTS

This work was supported by grants of the LUMC profile area "biomedical imaging" to H.E.K., A.W., and P.C.N.R; NWO-Veni (09150161910073) to M.R.B.; and the Netherlands Cardiovascular Research Initiative: an initiative with support of the Dutch Heart Foundation (CVON2017 GENIUS-2) to P.C.N.R.

DATA AVAILABILITY STATEMENT

Data are available from the corresponding author on reasonable request.

ORCID

Aashley S. D. Sardjoe Mishre https://orcid.org/0000-0002-8813-4876
Borja Martinez-Tellez https://orcid.org/0000-0001-8783-1859
Maaike E. Straat https://orcid.org/0000-0002-3148-8358
Mariëtte R. Boon https://orcid.org/0000-0002-3247-7538
Oleh Dzyubachyk https://orcid.org/0000-0003-1344-7189
Andrew G. Webb https://orcid.org/0000-0003-4045-9732
Patrick C. N. Rensen https://orcid.org/0000-0002-8455-4988
Hermien E. Kan https://orcid.org/0000-0002-5772-7177

REFERENCES

1. Blondin DP, Frisch F, Phoenix S, et al. Inhibition of intracellular triglyceride lipolysis suppresses cold-induced brown adipose tissue metabolism and increases shivering in humans. *Cell Metab.* 2017;25:438-447. doi:10.1016/j.cmet.2016.12.005
2. Bartelt A, Bruns OT, Reimer R, et al. Brown adipose tissue activity controls triglyceride clearance. *Nat Med.* 2011;17:200-206. doi:10.1038/nm.2297
3. Oikonomou EK, Antoniades C. The role of adipose tissue in cardiovascular health and disease. *Nat Rev Cardiol.* 2019;16:83-99. doi:10.1038/s41569-018-0097-6
4. Becher T, Palanisamy S, Kramer DJ, et al. Brown adipose tissue is associated with cardiometabolic health. *Nat Med.* 2021;27:58-65. doi:10.1038/s41591-020-1126-7
5. Van Der Lans AAJJ, Hoeks J, Brans B, et al. Cold acclimation recruits human brown fat and increases nonshivering thermogenesis. *J Clin Investig.* 2013;123:3395-3403. doi:10.1172/JCI68993
6. Yoneshiro T, Aita S, Matsushita M, et al. Recruited brown adipose tissue as an antiobesity agent in humans. *J Clin Invest.* 2013;123:3404-3408. doi:10.1172/JCI67803
7. Cannon B, Nedergaard J. Brown adipose tissue: function and physiological significance. *Physiol Rev.* 2004;84:277-359. doi:10.1152/physrev.00015.2003
8. Straat ME, Hoekx CA, van Velden FHP, et al. Stimulation of the beta-2-adrenergic receptor with salbutamol activates human brown adipose tissue. *Cell Rep Med.* 2023;4:100942. doi:10.1016/j.xcrm.2023.100942
9. Chen KY, Cypess AM, Laughlin MR, et al. Brown adipose reporting criteria in imaging STudies (BARCIST 1.0): recommendations for standardized FDG-PET/CT experiments in humans. *Cell Metab.* 2016;24:210-222. doi:10.1016/j.cmet.2016.07.014
10. Schilperoort M, Hoeke G, Kooijman S, Rensen PCN. Relevance of lipid metabolism for brown fat visualization and quantification. *Curr Opin Lipidol.* 2016;27:242-248. doi:10.1097/MOL.0000000000000296
11. Karampinos DC, Weidlich D, Wu M, Hu HH, Franz D. Techniques and applications of magnetic resonance imaging for studying Brown adipose tissue morphometry and function. *Handb Exp Pharmacol.* 2019;251:299-324. doi:10.1007/164_2018_158
12. Wu M, Junker D, Branca RT, Karampinos DC. Magnetic resonance imaging techniques for brown adipose tissue detection. *Front Endocrinol (Lausanne).* 2020;11:421. doi:10.3389/FENDO.2020.00421/FULL
13. Oreskovich S, Ong F, Ahmed B, et al. Magnetic resonance imaging reveals human brown adipose tissue is rapidly activated in response to cold. *J Endocr Soc.* 2019;14:2374-2384. doi:10.1210/js.2019‐00309
14. Deng J, Neff LM, Rubert NC, et al. MRI characterization of brown adipose tissue under thermal challenges in normal weight, overweight, and obese young men. *J Magn Reson Imaging.* 2018;47:936-947. doi:10.1002/jmri.25836
15. Coolbaugh CL, Damon BM, Bush EC, Welch EB, Towse TF. Cold exposure induces dynamic, heterogeneous alterations in human

brown adipose tissue lipid content. *Sci Rep.* 2019;9:13600. doi:10.1038/s41598-019-49936-x
16. Lundström E, Strand R, Johansson L, Bergsten P, Ahlström H, Kullberg J. Magnetic resonance imaging cooling-reheating protocol indicates decreased fat fraction via lipid consumption in suspected brown adipose tissue. *PLoS One.* 2015;10:e0126705. doi:10.1371/journal.pone.0126705
17. Gashi G, Madoerin P, Maushart CI, et al. MRI characteristics of supraclavicular brown adipose tissue in relation to cold-induced thermogenesis in healthy human adults. *J Magn Reson Imaging.* 2019;50:1160-1168. doi:10.1002/jmri.26733
18. Stahl V, Maier F, Freitag MT, et al. In vivo assessment of cold stimulation effects on the fat fraction of brown adipose tissue using DIXON MRI. *J Magn Reson Imaging.* 2017;45:369-380. doi:10.1002/jmri.25364
19. Reber J, Willershäuser M, Karlas A, et al. Non-invasive measurement of brown fat metabolism based on optoacoustic imaging of hemoglobin gradients. *Cell Metab.* 2018;27:689-701.e4. doi:10.1016/j.cmet.2018.02.002
20. Franz D, Diefenbach MN, Treibel F, et al. Differentiating supraclavicular from gluteal adipose tissue based on simultaneous PDFF and T_2^* mapping using a 20-echo gradient-echo acquisition. *J Magn Reson Imaging.* 2019;50(20):424-434. doi:10.1002/jmri.26661
21. Hu HH, Yokoo T, Bashir MR, et al. Linearity and bias of proton density fat fraction as a quantitative imaging biomarker: a multicenter, multiplatform, multivendor phantom study. *Radiology.* 2021;298:640-651. doi:10.1148/RADIOL.2021202912/ASSET/IMAGES/LARGE/RADIOL.2021202912.TBL6.JPEG
22. Wang X, Hernando D, Reeder SB. Sensitivity of chemical shift-encoded fat quantification to calibration of fat MR Spectrum. *Magn Reson Med.* 2016;75:845-851. doi:10.1002/MRM.25681
23. Klein S, Staring M, Murphy K, Viergever MA, Pluim JPW. Elastix: a toolbox for intensity-based medical image registration. *IEEE Trans Med Imaging.* 2010;29:196-205. doi:10.1109/TMI.2009.2035616
24. Abreu-Vieira G, Sardjoe Mishre ASD, Burakiewicz J, et al. Human brown adipose tissue estimated with magnetic resonance imaging undergoes changes in composition after cold exposure: an in vivo MRI study in healthy volunteers. *Front Endocrinol (Lausanne).* 2020;10:898. doi:10.3389/fendo.2019.00898
25. Wu M, Mulder HT, Baron P, et al. Correction of motion-induced susceptibility artifacts and B0 drift during proton resonance frequency shift-based MR thermometry in the pelvis with background field removal methods. *Magn Reson Med.* 2020;84:2495-2511. doi:10.1002/MRM.28302
26. Shcherbakova Y, van den Berg CAT, Moonen CTW, Bartels LW. Investigation of the influence of B0 drift on the performance of the PLANET method and an algorithm for drift correction. *Magn Reson Med.* 2019;82:1725-1740. doi:10.1002/MRM.27860
27. Hernandez D, Kim KS, Michel E, Lee SY. Correction of B0 drift effects in magnetic resonance thermometry using magnetic field monitoring technique. *Concepts Magn Reson Part B.* 2016;46B:81-89. doi:10.1002/CMR.B.21324
28. Kadoya N, Fujita Y, Katsuta Y, et al. Evaluation of various deformable image registration algorithms for thoracic images. *J Radiat Res.* 2014;55:175-182. doi:10.1093/JRR/RRT093
29. McCallister A, Zhang L, Burant A, Katz L, Branca RT. A pilot study on the correlation between fat fraction values and glucose uptake values in supraclavicular fat by simultaneous PET/MRI. *Magn Reson Med.* 2017;78:1922-1932. doi:10.1002/mrm.26589
30. Straat ME, Jurado-Fasoli L, Ying Z, et al. Cold exposure induces dynamic changes in circulating triacylglycerol species, which is dependent on intracellular lipolysis: a randomized cross-over trial. SSRN https://papers.ssrn.com/sol3/papers.cfm?abstract_id=4163695 Accessed July 20, 2022.

SUPPORTING INFORMATION

Additional supporting information may be found in the online version of the article at the publisher's website.

Figure S1. Normalized gradient correlation method was applied to first-echo magnitude images to compute the amount of displacement of each dynamic with respect to the first thermoneutral scan. This method consists in the Fourier shift theorem being applied to the gradient volumes. The gradient correlation map defines the probability of each possible displacement between the two volumes; in theory, in case the two volumes are exact shifted copies of each other, it will result in a single Dirac peak. The X, Y, and Z coordinates of the highest peak on this map correspond to the amount of shift in the X, Y, and Z directions of the dynamic image with respect to the reference one. The resulting displacement in the X-direction (columns; blue), Y-direction (rows; orange), and Z-direction (slices; green) is shown for all participants.

Figure S2. The influence of small positional changes caused by motion on supraclavicular brown adipose tissue (scBAT) fat fraction (FF) changes was determined by registering the first thermoneutral scan (reference scan) to each of its dynamics to mimic positional differences over time. For each time point, FF differences were calculated between the original reference scan's FF values and the deformed reference scan's FF values and averaged across the region of interest (ROI) in scBAT (A), the trapezius muscle (B), and the humerus bone (C). To evaluate whether our coregistration method could effectively resolve for motion-induced variability, we back-transformed each deformed reference scan to its original coordinates. For each time point, FF differences were calculated between the original reference scan's FF values and the back-transformed reference scan's FF values and averaged across the ROI in scBAT (D), the trapezius muscle (E), and the humerus bone (F).

Figure S3. Fat fraction (FF) changes are shown for nonregistered data after applying a 30%–100% single FF threshold (black) and mutual FF threshold (orange). Red boxes denote the thermoneutral period.

Figure S4. Absolute fat fraction (FF) during thermoneutrality and cooling as a function of decades. Voxels that fell within a certain decade (e.g., 0%–10% FF) were first extracted in the precooling scan. The same voxels were then also extracted in the last cooling dynamic. For both scans, FF values of the extracted voxels were averaged, yielding an absolute FF. The absolute FF is shown on the y-axis as a function of decades (e.g., 0%–10% FF) for the first thermoneutral scan (red) and the last cooling dynamic (blue). A Wilcoxon signed-rank test was used for analysis.

How to cite this article: Sardjoe Mishre ASD, Martinez-Tellez B, Straat ME, et al. Image registration and mutual thresholding enable low interimage variability across dynamic MRI measurements of supraclavicular brown adipose tissue during mild cold exposure. *Magn Reson Med*. 2023;90:1316-1327. doi: 10.1002/mrm.29707